

γ - γ Angular Correlation and Time-Integral Perturbed-Angular-Correlation Measurements on ^{28}Al

Neil Heiman and W. J. Kossler

College of William and Mary, Williamsburg, Virginia 23185

(Received 7 June 1972)

γ - γ angular correlation and time-integral perturbed-angular-correlation measurements involving low-lying levels of ^{28}Al have been performed. The 1343-30-keV, 943-30-keV, and 400-943-keV γ - γ angular correlations were studied simultaneously. The results conclusively establish the spin and parity assignments for the ground, 30-, 973-, and 1373-keV states to be 3^+ , 2^+ , 0^+ , and 1^+ , respectively. Analysis of the data indicates that the mixing amplitude for the $2^+ \rightarrow 3^+$ transition is $\delta(E2/M1) = -0.004 \pm 0.006$ and for the $1^+ \rightarrow 2^+$ transition $\delta(E2/M1) = +0.35 \pm 0.10$. The moment of the 2^+ state was determined by time-integral perturbed angular correlations to be $(+4.27 \pm 0.40) \mu_N$. The implications of this value for the systematics of magnetic moments in the vicinity of $A = 28$ are discussed particularly in relation to the theory of weak magnetism in β decay.

I. INTRODUCTION

Until very recently, only rudimentary spectroscopic information on the ^{28}Al nucleus was available. Only within the last year have detailed determinations of spins, parities, transition rates, and spectroscopic factors of low-lying levels in ^{28}Al been undertaken. The most recent publications include γ -ray spectroscopy and particle- γ -ray angular-correlation measurements of Boerma and Smith,¹ the electromagnetic transition rate measurements of Maher *et al.*,² the determination of spectroscopic factors from $^{27}\text{Al}(d, p)^{28}\text{Al}$ reaction by Maher *et al.*,³ and a preliminary report of γ - γ angular correlation by Lawergren.⁴

The present paper reports the results of three separate γ - γ angular-correlation measurements on low-lying levels of ^{28}Al and a time-integral perturbed-angular-correlation determination of the moment of the 30-keV 2^+ state of ^{28}Al . The results of these measurements are consistent with and extend the results of the works cited above.

Since in the simplest shell model the $1d_{5/2}$ subshell closes at ^{28}Si , ^{28}Al is believed to be relatively undeformed for s - d -shell nuclei and therefore provides an interesting testing ground for various nuclear models. Nilsson-model and recent shell-model calculations have already achieved a considerable degree of success in predicting many of the observed characteristics of ^{28}Al .^{2,5,6} The present paper combined with the other recent research on low-lying levels in ^{28}Al provide a considerable amount of detailed data on this nucleus which can provide the basis for refinement of the model calculations.

II. EXPERIMENTAL PROCEDURE

A. Source Production

The source for these experiments was the 21.3-h half-life β emitter ^{28}Mg . The source was produced in the reaction $^{30}\text{Si}(p, 3p)^{28}\text{Mg}$ by bombarding ^{30}Si in the form of SiO_2 with 300-MeV protons from the Space Radiation Effects Laboratory 600-MeV synchrocyclotron. 300 MeV was chosen with the hope of minimizing unwanted reactions. An expected difficulty encountered was the high yield of ^{24}Na . The amount of this activity produced varied with each irradiation but on the average was 20 times as intense as the ^{28}Mg . This much general background activity is undesirable in any experiment but is particularly a problem for this experiment since the 1369-keV γ ray from the decay of ^{24}Na is resolved from the 1343-keV γ ray of ^{28}Al only with a Ge(Li) detector. Since it was impractical from the standpoint of a number of considerations including counting efficiency to use a Ge(Li) detector and since the half-lives of ^{24}Na and ^{28}Mg are comparable, it became necessary to radiochemically extract the ^{28}Mg . Radiochemical separation was accomplished by dissolving the activated SiO_2 in concentrated HF. The ^{28}Mg was then precipitated in the form of MgF_2 by the addition of MgCl_2 . This procedure removed nearly 100% of the ^{28}Mg and only about 5% of the ^{24}Na . To avoid hyperfine interactions associated with the MgF_2 solid, the precipitate was redissolved in concentrated HNO_3 . For a few experimental data runs, the liquid was diluted with water and drained through a resin ion exchange column to further improve the radiochemical purity. This latter

procedure was essentially 100% effective in removing the ^{24}Na contamination; however, about 50% of ^{28}Mg was also lost. Since the level of activity was sufficiently low, prior to the ion exchange procedure, that background coincidences were not a problem, the ion exchange was judged undesirable because of large reduction in true counting that it produced.

B. Geometry

The relatively low counting rate required high-efficiency detectors. Therefore NaI counters were used. The three γ - γ angular correlations (1343-30-keV, 943-30-keV, and 400-943-keV) were investigated simultaneously. This not only provided the most efficient use of the source activity but also allowed a convenient method for cross checking and normalizing the data. A $1\frac{1}{2}$ -in. \times 1-in. NaI counter to detect the 30-keV γ ray was located at the 0° position of a circular table. A 3-in. \times 3-in. NaI counter to detect the 400-keV γ ray was located at the 270° position. A second 3-in. \times 3-in. NaI counter to detect both the 943- and the 1343-keV γ rays was placed on a movable arm which was programmed to move this detector between the 70° position and the 200° position. The detectors were magnetically shielded and well collimated. Collimation was a particularly serious consideration in this experiment since a 1343-keV γ ray could Compton scatter from one detector to another simulating a 400-943-keV coincidence, even when the electronics were set to detect only the photopeaks. Even with 1 cm of lead shielding between the detectors, these simulated coincidences gave rise to about a 5% anisotropy. To eliminate this effect, a 1.5-cm-thick lead shield with a 1.5-cm-thick conical lead collimator was placed around each detector for a total of 3.0 cm of lead shielding between detectors. The collimators tapered down to an opening diameter of 2.0 cm at a distance of 2.0 cm from the source. This system reduced the Compton scattering anisotropy to less than 0.5%.

To minimize the effect of any anisotropy in the distribution of the source, the source was spun about a central axis at 50 rpm.

C. Data Collection

The outputs of the NaI detectors were amplified and fed to the inputs of timing single-channel analyzers (SCA). Each SCA was set on the photopeak of its respective γ ray (either the 1343, 943, 400, or 30 keV). The fast outputs of the SCA's were fed pairwise to three fast-coincidence units, set to detect coincidences between the 400- and 943-keV γ rays, the 943- and 30-keV γ rays, and the

1343- and 30-keV γ rays. The timing resolution of this system was approximately 50 nsec, which was sufficient for the count rates involved.

The raw data consisted of the simultaneous collection of the four singles counting rates for the 30-, 400-, 943-, and 1343-keV γ rays and the three coincidence counting rates for the 943-30-keV, 1343-30-keV, and 400-943-keV coincidences. For some runs, data were collected every 10° as the movable detector was moved between 70° and 200° ; for other runs, data were collected every 30° between 90° and 180° . Examples of coincidence counting rates for the three γ - γ angular correlations are shown in Figs. 1 through 3. Several runs were performed. The data displayed in Figs. 1 through 3 were selected to illustrate the different manners in which data were collected and also, in the case of Fig. 3, to illustrate the dependence of the correlation on the source-to-detector distance. This latter point will be discussed below.

III. ANALYSIS OF THE DATA

The data were ultimately fitted to γ - γ angular-correlation theory. The expressions to which the data were fitted can be written in a number of ways. Since the data neither required nor found statistical significance to P_4 terms, these expressions take on the following simple forms:

$$\begin{aligned} W(\theta) &= 1 + A_{22}P_2(\cos\theta) \\ &= 1 + a_2 \cos^2\theta \\ &= 1 + b_2 \cos 2\theta \end{aligned}$$

defining the correlation coefficients A_{22} , a_2 , and b_2 . Furthermore A_{22} can be factored into two components, each of which depends upon only one of the γ rays in the cascade, i.e., $A_{22} = A_2(\gamma_1)A_2(\gamma_2)$. Completing the description of the notation, the anisotropy A is defined as $A = [W(180^\circ) - W(90^\circ)]/W(90^\circ)$.

Before fitting the data, it was necessary to correct for systematic anisotropies, finite solid angle, background, and accidental coincidences, extra-

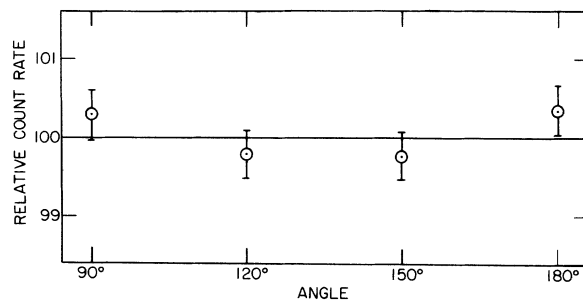


FIG. 1. Uncorrected relative number of 943-400-keV γ - γ coincidences as a function of angle between detectors.

nuclear interactions, and self-absorption in the source. The uncertainty associated with the correction for self-absorption was approximately 0.005 and proved to be the most significant factor limiting the accuracy of the determination of the true correlation coefficients. For comparison the statistical uncertainty in the correlation coefficients for each run was always less than 0.002.

The isotropic 943-400-keV correlation combined with the singles count rates provided a convenient check against systematic anisotropies. Experimentally this isotropic correlation exhibited an approximately 0.5% increase in count rate at 90 and 180° relative to 135°. By varying the thickness of the lead shielding and the diameter of the collimators, it became apparent that this anisotropy was due to the Compton scattering of the 1343-keV γ rays. This situation pertains to the 943-400-keV correlation only and cannot produce spurious coincidences in the case of either the 1343-30-keV or the 943-30-keV correlation. It is possible for a 1343-30-keV coincidence to be recorded as a 943-30-keV coincidence if the 1343-keV γ ray Compton scatters from the NaI detector depositing only 943 keV; but since the probability of this occurrence is small and the difference between the 943-30-keV correlation and the 1343-30-keV correlation is only about 4%, the effect of such a process may be neglected. The conclusion from these considerations and the experimental cross checks is that compared with the known uncertainty due to self-absorption other systematic errors were negligible.

The number of background coincidences can be determined from the single counting rates. This can also be determined experimentally by introducing a large delay between the inputs to the coincidence units. The two approaches yielded the same number so that this number could be con-

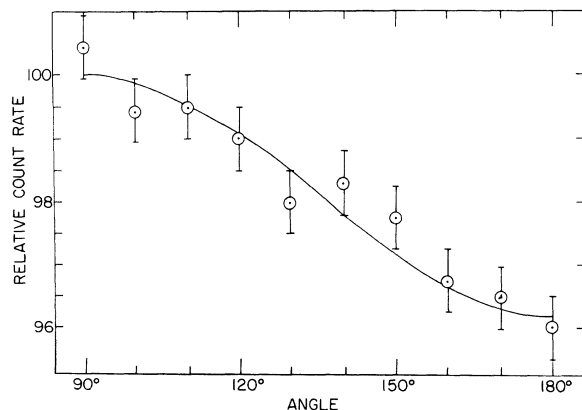


FIG. 2. Uncorrected relative number of 1343-30-keV γ - γ coincidences as a function of angle between detectors.

sidered reliable.

The radiochemical separation procedure yields a source in the form of MgF_2 . The extranuclear perturbations in this noncubic crystal are unknown. The approach taken to remove the unknown and undesirable effects of the extranuclear interactions was to dissolve the MgF_2 in concentrated HNO_3 . In order to insure these interactions were minimized, enough HNO_3 was used so that the viscosity of the solution was close to that of pure HNO_3 . This required approximately 1 ml of HNO_3 . Angular correlations were also measured with the source in the form of solid MgF_2 . In these runs, the angular-correlation coefficients tended to be roughly 0.02 less than with liquid sources [i.e., $|a_2(\text{solid})| \approx |a_2(\text{liquid})| - 0.02$]. The smallness of the attenuation due to solid-state effects suggests that any residual attenuation in the liquid sources was very small and could be safely neglected.

By using a liquid source, the problem of unknown extranuclear interactions is traded for the problem of enhanced self-absorption of the γ rays; but this latter effect can at least be calculated. Self-absorption is not significant for the 400-943-keV correlation but is critical for the two correlations involving the 30-keV γ ray. The main contribution to this source of error is not the mass absorption itself, but rather the combination of mass absorption and finite source size. This combination produces an effective detector solid angle which is a function of the angle between detectors. This problem has been treated in the literature,⁷ but no simple or easily applied correction formula exists. The size of this anisotropy depends upon the mass absorption coefficient, the dimensions of the source and the source-to-detector distance.

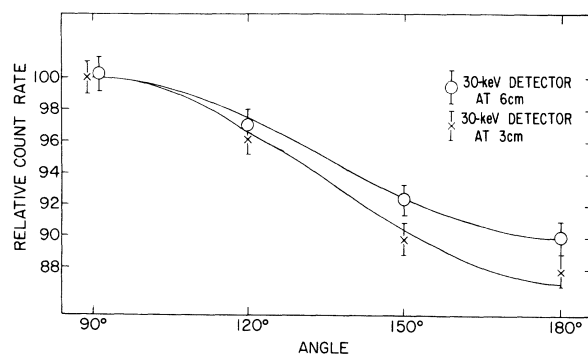


FIG. 3. Uncorrected relative number of 943-30-keV γ - γ coincidences as a function of angle between detectors. The two sets of data display the effect of γ -ray self-absorption in the source: The data with the lower anisotropy were taken with a source-to-detector distance of 3 cm. For the data with the larger anisotropy, this distance was 6 cm.

The mass absorption coefficient was measured experimentally. An approximate correction was then numerically calculated by dividing the source into a cylindrical grid and calculating the contribution of each sector and summing these contributions. The calculation was repeated for several different source dimensions and source-to-detector distances. The approximate validity of these calculations was checked experimentally by measuring the angular correlations as a function of these variables. The agreement between calculated and experimental values was very good. For example, Fig. 3 shows two measurements of the 943-30-keV correlation. The correlation with the larger anisotropy ($A \approx 0.12$) was taken with a source to detector distance of 3 cm; for the correlation with the lower anisotropy ($A \approx 0.10$) this distance was 6 cm. The calculated correction to the anisotropy A for the first case was 0.048 and for the second case was 0.028 yielding a difference in A of 0.020 between the two measurements which is in agreement with the observed difference. Similar agreement was obtained for the other correlation and when the diameter of the source was varied.

The remaining correction to be discussed is for the finite solid angle of the detectors. These corrections have been previously tabulated. The values used for this experiment are those published by Yates.⁸

IV. RESULTS OF γ - γ ANGULAR-CORRELATION MEASUREMENTS

When all the corrections are properly applied, the final values for the A_{22} coefficients are:

- (1) for the 400-943-keV correlation $A_{22} = 0.000 \pm 0.002$,
- (2) for the 943-30-keV correlation $A_{22} = -0.069 \pm 0.003$,
- (3) for the 1343-30-keV correlation $A_{22} = -0.039 \pm 0.012$.

The data were sufficiently unambiguous, even before applying the various corrections, to allow a conclusive assignment of spins and parities to the nuclear states. The assignments are:

- (1) ground state, $J^\pi = 3^+$;
- (2) 30-keV state, $J^\pi = 2^+$;
- (3) 973-keV state, $J^\pi = 0^+$;
- (4) 1371-keV state, $J^\pi = 1^+$.

These assignments are in agreement with previously suggested most probable values.^{1,2,9-11} Of these four states, only the spin and parity of the 973-keV level was seriously in doubt. The recent particle- γ correlations of Boerma and Smith¹ and the evidence outlined by Maher *et al.*² strongly suggested an assignment of 0^+ . The present experiment supplies doubly conclusive evidence of the correctness of this assignment, since the 0^+ level is involved in both the 943-400-keV correlation and the 943-30-keV correlation. Both of these required an assignment of 0^+ to fit the data. Furthermore, the results are clearly not consistent with other even remotely plausible spin, parity, and multipole mixing ratio. For example, the next most probable spin-parity assignment for the 973-keV state is 1^- . For unmixed multipolarities, this assignment predicts $A_{22} = -0.025$ for the 400-943-keV correlation and $A_{22} = +0.050$ for the 943-30-keV correlation. These predictions are clearly

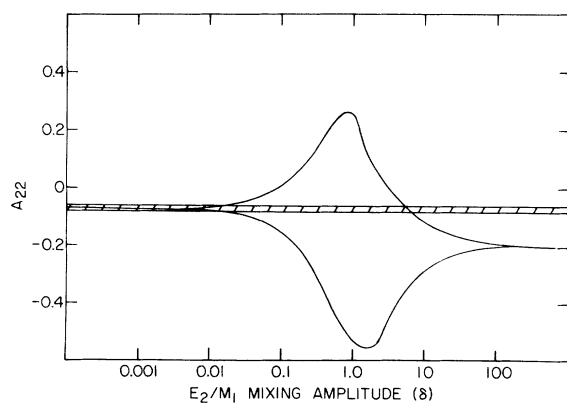


FIG. 4. The angular-correlation coefficient A_{22} for the 943-30-keV correlation as a function of E_2/M_1 mixing amplitude $\delta(E_2/M_1)$. The upper curve is the result for negative δ ; the lower for positive δ . The cross-hatched area indicates the experimental limits on A_{22} .

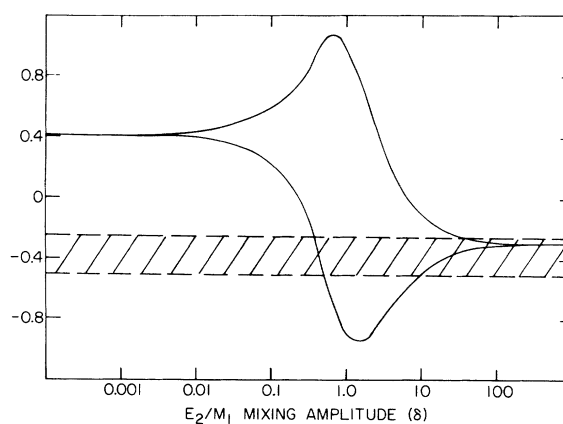


FIG. 5. The A_2 coefficient for the 1343-keV γ ray as a function of the E_2/M_1 mixing amplitude $\delta(E_2/M_1)$. The upper curve is the result for negative δ ; the lower for positive δ . The cross-hatched area indicates the experimental limits on A_2 .

at variance with the experimental results.

Since J^π for the 973-keV level is definitely 0^+ , the 943-keV γ ray is exclusively an $E2$ transition. Therefore the $E2/M1$ mixing amplitude $\delta(E2/M1)$ for the 30-keV γ ray can be extracted directly from the 943-30-keV correlation. The experimentally determined value is $\delta(E2/M1) = -0.004 \pm 0.006$ or $\delta(E2/M1) = -6.0 \pm 0.05$. (See Fig. 4.) The latter possibility can be ruled out on the basis of spin assignment, energy, and lifetime of the 30-keV state. The measured half-life of 30-keV state is 1.91 ± 0.08 nsec¹² and is consistent with a pure $M1$ transition. The value quoted here [$\delta(E2/M1) = -0.004 \pm 0.006$] agrees well with the value quoted by Boerma and Smith¹ [$\delta(E2/M1) = +0.03 \pm 0.05$].

All these values are consistent with $\delta(E2/M1) = 0$ as is the theoretical prediction of the modified shell-model calculations reported by Maher *et al.*²

A determination of $\delta(E2/M1)$ for the 1343-keV γ ray is less accurate for two reasons. First the 1343-30-keV correlation data were less precise, and secondly the uncertainty in the mixing amplitude of the 30-keV γ ray contributes to the uncertainty in the mixing amplitude of the 1343-keV γ ray. When the A_2 for the 30-keV γ ray was factored out of the A_{22} for 1343-30-keV correlation, the resulting A_2 for the 1343-keV γ ray was $A_2 = -0.35 \pm 0.10$. From Fig. 5 it can be seen that this corresponds to $\delta(E2/M1) = +0.35 \pm 0.10$ or $|\delta(E2/M1)| > 10$. This latter value cannot be ruled out completely; but, based on all the existing data, it is highly unlikely. The value $\delta(E2/M1) = +0.35 \pm 0.10$ is slightly higher than but consistent with the value quoted by Boerma and Smith¹ of $\delta(E2/M1) = +0.25 \pm 0.12$. Furthermore, combining this mixing amplitude with the electromagnetic transition rate measurement of Maher *et al.*,² one can determine the values of $B(M1)$ and $B(E2)$ for the 1343-keV γ ray. The results, $B(M1) = 0.039$ and $B(E2) = 6.32$, agree extremely well with the theoretical values [$B(M1) = 0.05$ and $B(E2) = 6.20$] obtained from the shell-model calculations of Maher *et al.*²

V. PERTURBED ANGULAR CORRELATION

To determine the magnetic moment of the 2^+ state, time-integral perturbed-angular-correlation measurements were performed with the application of a 7-kG magnetic field. The major source of uncertainty for this measurement turned out not to be statistics or experimental errors, but rather the uncertainty in the value of the unperturbed correlation coefficient. For this reason, most of the experimental effort was expended on measuring the precession of the much better determined 943-30-keV correlation. Measurements were also taken on the precession of the 1343-30-

keV correlation but only to check the correctness of the 943-30-keV data. Data for the precession of the 943-30-keV correlation were collected by two different methods. In the first method, the full angular correlation was measured in a manner identical to the method used to obtain the data in Figs. 1 to 3 except that a 7-kG field from a permanent magnet (with \vec{H} perpendicular to the plane of the detectors) was applied to the source. The field was reversed, and the experiment repeated. An advantage of this method was that the data could be normalized to the isotropic 943-400-keV correlation. A seeming further advantage is that the magnitude of b_2 as well as the precession angle ϕ could have been measured at the same time; however, the measurement of b_2 is subject to the same uncertainties as were present in the unperturbed correlation measurements, so little is to be gained in this regard. The serious disadvantage of this method of data collection is that it is inefficient in that too much time is spent collecting data at angles where the data is not sensitive to the perturbation. The second approach, which constituted a much more efficient use of the source, consisted of placing two fixed 3-in. \times 3-in. NaI counters to detect 943-keV γ rays symmetric about the 180° position at 140° and 220° , with a fixed $1\frac{1}{2}$ -in. \times 1-in. NaI counter at 0° to detect the 30-keV γ rays. The drawback of this approach is that normalization of the data and checking for systematic error are a little more difficult. On the other hand since, unlike the first method, the geometry is not changed with time, normalization and systematic errors are much less a problem. Normalization to singles counting rates and to average coincidence counting rates were self-consistent and judged therefore to be a satisfactory

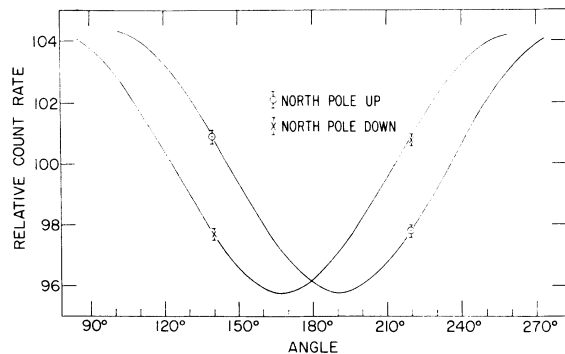


FIG. 6. The normalized 943-30-keV counting rate with 140° and 220° between counters as a function of the polarity of a 7.0-kG magnetic field. The solid lines are fits to the function

$$W(\theta, \infty, B) = 1 + \frac{b_2 \cos 2(\theta - \phi)}{[1 + (\tan 2\phi)^2]^{1/2}}.$$

procedure.

Results of data acquired by this method are displayed in Fig. 6. The data were corrected for background and fit by a successive approximation technique to the function:

$$W_{\perp}(\theta, \infty, B) = 1 + \frac{b_2 \cos 2(\theta - \phi)}{[1 + (\tan 2\phi)^2]^{1/2}}.$$

To determine ϕ , b_2 was held fixed at the value determined by the unperturbed 943-30-keV correlation. The resulting fit yielded $\phi = 10.8 \pm 0.7^\circ$. If the current best value for the half-life of the 2^+ state of 1.91 ± 0.08 nsec¹² is used, the precession angle corresponds to a nuclear moment of $(4.27 \pm 0.40) \mu_N$. The precession angle obtained by measuring the full correlation (the first method described) corroborates the value quoted above; but, because data accumulation was less efficient, the uncertainty is about twice as large. Measurement of the precession of the 1343-30-keV correlation also corroborates this value but the uncertainty is even larger.

VI. DISCUSSION

The 3^+ ground state of ^{28}Al and the 2^+ state, the magnetic moment of which is reported in this paper, form a doublet which can be thought to be composed of the $\frac{5}{2}^+$ ground state of ^{27}Al and the $\frac{1}{2}^+$ ground state of ^{29}Si . The magnetic moments for both these states are known and can be used to predict the ^{28}Al moments. In another model, namely the simplest shell model, the $\frac{5}{2}^+$ state is a $1d_{5/2}$ proton hole and the $\frac{1}{2}^+$ state is a $2s_{1/2}$ neutron particle. If free or Dirac values are chosen for the spin- g factors, one obtains other magnetic moments. The magnetic moments for the 3^+ and 2^+ states as well as $B(M1)$ for the $2^+ \rightarrow 3^+$ transition for all three choices are presented in Table I.

TABLE I. Moments and $B(M1)$ for ^{28}Al . Underlined numbers are experimentally determined values. Moments for ^{27}Al and ^{29}Si have been taken from the compilation of V. S. Shirley in *Hyperfine Interactions in Excited Nuclei*, edited by G. Goldring and R. Kalish (Gordon and Breach, New York, 1971), p. 1255.

		Present work	^{27}Al - ^{29}Si	Free	Dirac
μ^{3+}	(μ_N)	+4.16 ^a	+3.09	+2.88	+3
μ^{2+}	(μ_N)	<u>+4.27</u>	+3.77	+5.74	+3.80
$B(M1)$	$(\mu_N)^2$	<u>0.71</u>	0.91	4.58	0.20
$\mu_{5/2}^P$	(μ_N)	+4.42	<u>+3.64</u>	+4.79	3
$\mu_{1/2}^N$	(μ_N)	-0.25	<u>-0.55</u>	-1.91	0

^a This value and other numbers in this column that are not underlined have been calculated using the experimentally determined μ^{2+} and $B(M1)$.

The moments are related by: $\mu_{3^+} = \mu_{5/2^+} + \mu_{1/2^+}$, $\mu_{2^+} = \frac{1}{15} \mu_{5/2^+} - \frac{2}{3} \mu_{1/2^+}$, and

$$B(M1) = \frac{7}{4\pi} \left[\frac{\mu_{5/2^+}}{5} + \mu_{1/2^+} \right]^2.$$

The $B(M1)$ has been measured and together with the 2^+ magnetic moment reported here may be used to obtain the $\frac{5}{2}^+$ and $\frac{1}{2}^+$ magnetic moments and from these the 3^+ moment. These are also presented in Table I. It seems clear that the measured 2^+ moment and $B(M1)$ agree quite reasonably with values based on the moments of ^{27}Al and ^{29}Si . The agreement is certainly better than for the case using the free or Dirac $d_{5/2}$ and $s_{1/2}$ moments. This is to be expected since the ^{27}Al - ^{29}Si system already includes most of the wave-function admixtures found in ^{28}Al .

The 3^+ and 2^+ states of ^{28}Al , ^{28}Si , and ^{28}P form isotriplets. The moments of these states are related to the weak magnetism contribution to the superallowed β decay of ^{28}P .¹³ Information is not yet sufficient for direct prediction in this matter without additional assumptions. Several choices present themselves. One can assume a $d_{5/2}$ - $s_{1/2}$ configuration and use free, Dirac, or ^{27}Al - ^{29}Si values for the spin- g factors. The assumption most likely to be successful would be to use the ground state of ^{29}P for the $\frac{1}{2}^+$ configuration and ^{27}Si for the $\frac{5}{2}^+$. Unfortunately the ^{27}Si moment is not known. ^{25}Mg , with two additional proton holes predominantly coupled to zero angular momentum, should have a moment which does not differ greatly from that of ^{27}Si . The small effect of two additional particles can be seen, for example, in the comparison of the moments of ^{29}P and ^{31}P . The moments and $B(M1)$ for ^{28}P based on the various assumptions are presented in Table II. Considering the success of the neighboring nuclei prediction for ^{28}Al and the near equality of the ^{29}P and ^{31}P moments, one should expect the ^{25}Mg - ^{29}P predic-

TABLE II. Moments and $B(M1)$ ^{28}P . All new moments listed here are derived as described in the text. Moments of ^{25}Mg and ^{29}P were taken from the same source as those of ^{27}Al and ^{29}Si of Table I.

		Present work	^{25}Mg - ^{29}P	^{27}Al - ^{29}Si	Free	Dirac
μ^{3+}	(μ_N)	2.16	0.28	1.08	0.88	1
μ^{2+}	(μ_N)	-1.85	-1.55	-1.61	-3.64	0.66
$B(M1)$	$(\mu_N)^2$	3.40	0.94	1.71	5.60	1
$2^+ \rightarrow 3^+$						
$\mu_{5/2}^N$	(μ_N)	-0.25	-0.85	-0.55	-1.91	0
$\mu_{1/2}^P$	(μ_N)	2.42	1.13	1.64	2.79	1

tion to be correct to within 20–30%.

The present results suggest several other experiments. Determination of the magnetic moment of ^{27}Si would allow better prediction of the ^{28}P moments. The moment of the 3^+ ground state of ^{28}Al should be as well predicted as that of the 2^+ state, and a confirmation would be encouraging. [Note added in proof: This moment has now been measured¹⁴: $\mu_{3^+} = (2.789 \pm 0.001)\mu_N$.] The $M1$ rate between the 3^+ - 2^+ doublet of ^{28}P and the moments of both states would provide an interesting test and comparison of the assumption that ^{25}Mg - ^{29}P provide the basic moment information. The magnetic moments of the 3^+ states of ^{28}P and ^{28}Al are related by the assumption of a conserved vector current (CVC) to the weak magnetism contribution to the β decay from the 3^+ , $T=1$ analog state in

^{28}Si . By detailed study of this β decay one can separately obtain the weak magnetism contribution for comparison. It should be noted that the value of the magnetic moment for the 3^+ state in ^{28}P based on the moments of ^{25}Mg and ^{29}P , which the above analysis indicates is most appropriate, is markedly smaller than that based on the other assumptions. With this moment, the isovector contribution to the moments of the istriplet ($\mu_3 = \mu_{^{28}\text{Al}^{3^+}} - \mu_{^{28}\text{P}^{3^+}}$) is 2.81 in contrast to a value of $\mu_3 = 2$ based on the free or Dirac g factors and simple wave functions. Since the weak magnetism term would be expected to go with the isovector magnetic moment, this result indicates that the weak magnetism amplitude may be larger than might have been expected.

¹D. O. Boerma, Ph.D. thesis, Ryksuniversitet Groningen, 1970 (unpublished); D. O. Boerma and P. B. Smith, Phys. Rev. C 4, 1200 (1971).

²J. V. Maher, G. B. Beard, G. H. Wedberg, E. Sprenkel-Segel, A. Yousef, B. H. Wildenthal, and R. E. Segel, Phys. Rev. 5, 1322 (1972).

³J. V. Maher, H. T. Fortune, G. C. Morrison, and B. Ziedman, Phys. Rev. C 5, 1313 (1972).

⁴B. Lawergren, Bull. Am. Phys. Soc. 17, 90 (1972).

⁵R. K. Sheline, Nucl. Phys. 2, 382 (1956).

⁶R. J. Ascitutto, D. A. Bell, and J. P. Davidson, Phys. Rev. 176, 1323 (1968).

⁷E. Breitenberger, Proc. Phys. Soc. (London) A67,

1108 (1954).

⁸M. J. L. Yates in *Alpha-, Beta-, and Gamma-Ray Spectroscopy*, edited by K. Siegbahn, (North-Holland, Amsterdam, 1965), Vol. II, p. 1691.

⁹D. E. Alburger and W. R. Harris, Phys. Rev. 185, 1495 (1969).

¹⁰P. M. Endt and C. Van de Leun, Nucl. Phys. A105, 1 (1967).

¹¹B. Lawergren, Nucl. Phys. A96, 49 (1967).

¹²D. Bloess, A. Krusche, and F. Mümmich, Z. Physik 192, 358 (1966).

¹³M. Gell-Mann, Phys. Rev. 111, 362 (1958).

¹⁴H. Lades, Z. Physik 252, 242 (1972).